Archives of Virology 59, 25—33 (1979)

Archives of Virology

Comparison of the Morphology of Three Coronaviruses

By

Heather A. Davies and M. R. Macnaughton

Section of Electron Microscopy and Division of Communicable Diseases,
Clinical Research Centre,
Harrow, Middlesex, England

With 3 Figures

Accepted August 22, 1978

Summary

The morphology of three coronaviruses; avian infectious bronchitis virus strain Connecticut (IBV Conn), human coronavirus strain 229E (HCV 229E) and mouse hepatitis virus strain 3 (MHV3), were examined by negative staining. Significant differences were found in the sizes of the three coronaviruses. Furthermore, three types of surface projection of the same lengths, but varying widths and morphology, were observed. Both IBV Conn and HCV 229E had bulbous projections characteristic of coronaviruses, although the projections of HCV 229E were somewhat thinner than those of IBV Conn. On the other hand, MHV3 particles had thin, cone-shaped surface projections, that were completely unlike typical coronavirus projections. The significance of these results is discussed.

Introduction

Coronaviruses are a group of lipid-containing RNA viruses that have a unique morphology (15, 22). The virions are usually described as being large pleomorphic spherical particles with characteristic bulbous, widely-spaced surface projections that form a corona around the particles (15). The virus envelope contains lipid and appears to consist of a distinct pair of electron dense shells (15) and a single-stranded helical internal component that has been identified as ribonucleoprotein (10). At present, coronaviruses are classified almost entirely by means of their characteristic morphology, and although preliminary biochemical and serological criteria are now available for some coronaviruses (22), the relative difficulty in isolating and growing some of these viruses in cell culture for biochemical analysis means that for some time it will be necessary to classify many coronaviruses entirely by their morphological features.

Measurements of the sizes of various coronavirus species by different investigators using negative staining have revealed a large range in total diameters

0304-8608/79/0059/0025/$ 01.80

of between 50 and 220 nm, with average total diameters ranging from 75 to 160 nm (15). Furthermore, the bulbous surface projections vary in shape and size, with lengths of between 12 and 24 nm (15). Few measurements of the width of these projections have been made. In some cases, long, thin, rod-like surface projections of length approximately 20 nm have been observed that bear little if any resemblance to 'typical' coronavirus projections (1, 3, 4, 16). Sometimes spherical dilations or T-shaped structures were observed at the distal end of these projections.

As no previous comparative studies have been made on the detailed structure of different coronaviruses, we have analysed the morphology by negative staining of three coronaviruses: avian infectious bronchitis virus strain Connecticut (IBV Conn), human coronavirus strain 229E (HCV 229E) and mouse hepatitis virus strain 3 (MHV3). The results we have obtained are of importance in the morphological classification of coronaviruses.

Materials and Methods

Virus Growth

IBV strain Connecticut (IBV46) was grown in 10-day old embryonated chicken eggs incubated at 37° C for 24 hours as previously described (11). HCV229E was grown in monolayer cultures of embryo lung cells of the MRC continuous line at 33 °C for 32 hours in Eagles' BME with 2 per cent new born calf serum (13). MHV3 was grown in confluent secondary mouse embryonic fibroblasts at 37° C for 72 hours in Eagles' MEM with 2 per cent foetal calf serum (10). Cell cultures containing HCV229E and MHV3 particles were frozen and thawed three times and then purified.

Virus Purification

All the purification steps were performed at 0° to 4° C. The virus suspension was clarified at $2000 \times g$ for 30 minutes, pelleted at $75{,}000 \times g$ for 1 hour and then resuspended in 1 ml Dulbecco's phosphate buffered saline 'A' (PBSA). The resuspended virus was overlaid on to a linear 25 to 55 per cent (w/w) sucrose gradient in PBSA and centrifuged for 16 hours at $90{,}000 \times g$. The virus peak at 1.18 g/ml was collected, diluted in PBSA and again layered onto a linear 25 to 55 per cent (w/w) sucrose gradient in PBSA and centrifuged for 16 hours at $90{,}000 \times g$. Peak fractions at 1.18 g/ml were examined by electron microscopy.

Electron Microscopy

One aliquot of each virus sample was negatively stained with 2 per cent (w/v) potassium phosphotungstate pH 6.5 and a second with 0.5 per cent (w/v) uranyl acetate, pH 4.4, and examined in a Philips EM300 electron microscope. Three features of coronavirus morphology were examined, namely, the envelope diameter (excluding surface projections) and the length and width of the surface projections. Approximately 50 envelope diameters of each virus species were measured. In each case two measurements of diameter were taken and the average value was used in subsequent calculations. For elliptical shaped virus particles, one measurement was taken across the long axis and the other across the short axis (18). Between 50 and 100 measurements of surface projection lengths and widths were made for each virus species. Lengths were measured from the boundary of the virus envelopes to the distal end of the projections and widths were measured at the widest parts of the projections. An analysis of variance was performed on the measurements for each feature, using each staining method, to determine whether the means for the three viruses differed significantly.

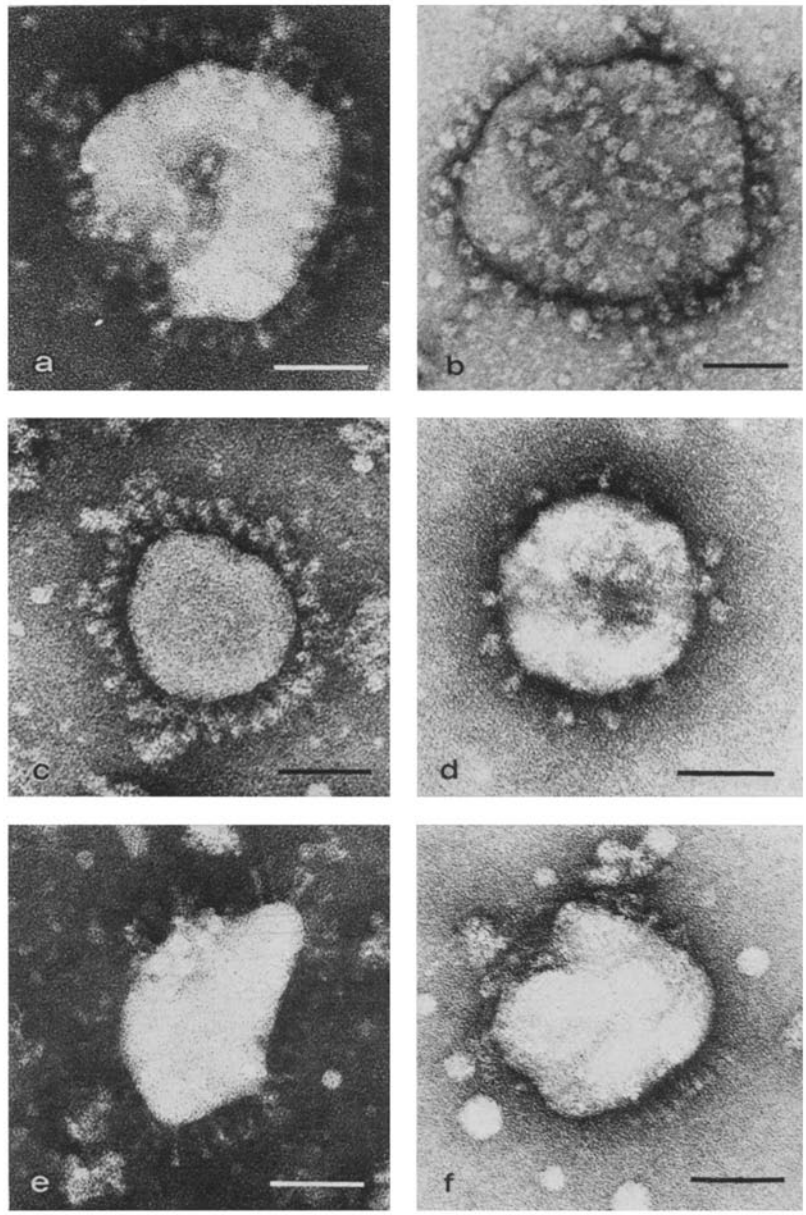

Fig. 1. Negatively stained preparations of purified coronavirus particles. *a* IBV Conn stained with 2 per cent potassium phosphotungstate, pH 6.5; *b* IBV Conn stained with 0.5 per cent uranyl acetate, pH 4.4; *c* HCV 229 E stained with 2 per cent potassium phosphotungstate, pH 6.5; *d* HCV 229 E stained with 0.5 per cent uranyl acetate, pH 4.4; *e* MHV 3 stained with 2 per cent potassium phosphotungstate, pH 6.5; *f* MHV 3 stained with 0.5 per cent uranyl acetate, pH 4.4. The bar represents 50 nm

Results

Virus Purification and Morphology

Purified coronavirus particles of density 1.18 g/ml from sucrose gradients were examined in this study as only these particles comprised complete infectious particles (MACNAUGHTON, manuscript in preparation). Nevertheless, the morphology of virus particles of other densities was similar to that of the complete particles. Figure 1 shows electron micrographs of IBV Conn, HCV 229E and MHV3 examined by negative staining with potassium phosphotungstate (KPT) and uranyl acetate (UA). Typical, more or less spherical coronavirus particles were observed with almost complete coronas of surface projections. The particles remained intact with both negative stains as judged by the exclusion of stain from them.

Variations in Size

Table 1 summarises the results of measurements of envelope diameters of IBV Conn, HCV 229E and MHV3 using purified virus preparations, negatively stained with KPT or UA. For each stain IBV Conn was highly significantly greater than the other two ($p<0.001$), while the other two were less, but still significantly, different from each other. IBV Conn and MHV3 showed no significant difference as between one stain and the other, but HCV 229E had a highly significantly greater diameter ($p<0.001$) when stained with UA than when stained with KPT. With KPT staining MHV3 had a larger average diameter then HCV 229E ($p=0.001$), while the reverse was true for UA staining ($0.005>p>0.001$).

Table 1. *Diameters of the envelopes of three coronaviruses determined using different negative stains*

Coronavirus species	Potassium phosphotungstate diameters (nm)[a]				Uranyl acetate diameters (nm)[b]			
	Number of observations	Mean	Standard error	Range	Number of observations	Mean	Standard error	Range
IBV Conn	41	129.5	3.8	90—197	52	125.9	2.5	90—171
HCV 229E	49	89.6	1.5	67—123	61	108.9	2.3	75—152
MHV3	41	96.5	1.3	78—116	47	100.0	1.7	76—121

[a] Negative staining with 2 per cent potassium phosphotungstate, pH 6.5
[b] Negative staining with 0.5 per cent uranyl acetate, pH 4.4

Figure 2 shows histograms of the envelope diameters of the three coronaviruses stained with KPT. Most HCV 229E and MHV3 particles had envelope diameters showing little spread around the mean values. However, there was a wider spread in the diameters of IBV Conn envelopes. The diameters of UA stained virus envelopes were distributed as in Figure 2 (not shown), except for HCV 229E (Table 1).

Morphology of the Surface Projections

Three types of surface projections were found. Those of IBV Conn (Fig. 1a and b) and HCV 229E (Figs. 1c and d) were bulbous or 'tear-drop' shaped and

were widely spaced on the virus envelope. However, those of MHV3 (Figs. 1e and f) were 'cone-shaped' with the thicker, flat part at the distal end. They were spaced closely together on the virus envelope though not as many particles exhibited complete coronas as IBV Conn and HCV 229E.

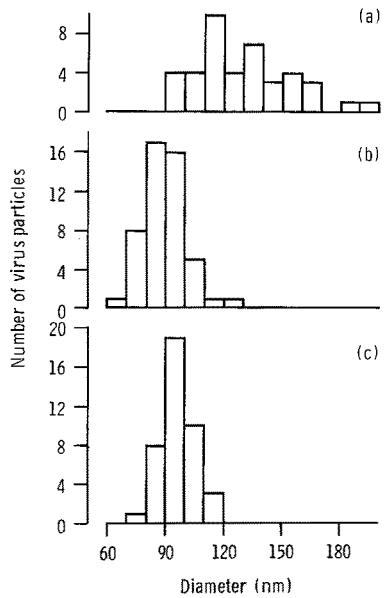

Fig. 2. Histograms of the envelope diameters of three coronaviruses determined using negative staining with 2 per cent potassium phosphotungstate, pH 6.5. *a* IBV Conn, *b* HCV 229E and *c* MHV3

Table 2. *Lengths of the surface projections of three coronaviruses determined using different negative stains*

Coronavirus species	Potassium phosphotungstate lengths (nm)[a]				Uranyl acetate lengths (nm)[b]			
	Number of observations	Mean	Standard error	Range	Number of observations	Mean	Standard error	Range
IBV Conn	70	19.8	0.35	12.8—27.3	64	14.1	0.24	9.7—19.1
HCV 229E	89	20.3	0.19	15.6—23.8	88	10.9	0.29	7.2—19.5
MHV3	104	19.7	0.15	16.6—23.4	53	18.5	0.30	13.3—23.4

[a] Negative staining with 2 per cent potassium phosphotungstate, pH 6.5
[b] Negative staining with 0.5 per cent uranyl acetate, pH 4.4

In spite of this difference in shape, the values of length shown in Table 2 were not found to be significantly different from each other when KPT staining was used. However, with UA staining, the three types were highly significantly different from each other ($p<0.001$), and all three were considerably shortened compared with their KPT values ($p<0.001$ in each case).

Figures 3a and b show histograms of the lengths of the projections of IBV Conn and HCV 229E respectively, determined from KPT stained preparations. It is of interest to note that the lengths of the projections of IBV Conn show a much greater spread in values than HCV 229E, but this difference in spread is not sufficient to invalidate the analysis of variance. The spread of lengths of projections of IBV Conn in UA stained preparations was similar to that obtained using KPT but HCV 229E and MHV3 had a wider spread with UA than with KPT (not shown). In one preparation of HCV 229E, projections were observed that were not consistent with the above description. A small percentage of particles in this preparation had projections that were thinner than the 'tear-drop' morphology, being 17 to 24 nm long and 3.9 to 5.6 nm wide. Projections of this type were not seen in preparations of IBV Conn.

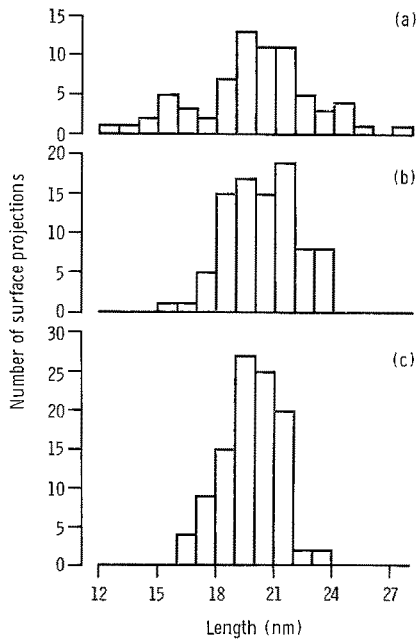

Fig. 3. Histograms of the lengths of the surface projections of three coronaviruses determined using negative staining with 2 per cent potassium phosphotungstate, pH 6.5. *a* IBV Conn, *b* HCV 229E and *c* MHV3

Figure 3c shows a histogram of the spread of values using KPT for the length of MHV3 surface projections. The spread was similar to that determined from UA treated preparations (not shown) and to KPT treated HCV 229E preparations (Fig. 3b). In three preparations of MHV3, negatively stained with KPT a small percentage of the surface projections did not have the 'cone-shaped' morphology. These were bulbous in shape, 7.5 to 14 nm long and 6 to 11 nm wide.

Table 3 shows the widths of the surface projections. Here the main difference lies in the MHV3 values being smaller than the others, while the IBV Conn values were a little greater than the HCV 229E values, and for each virus species the values using UA were rather greater than those using KPT ($p<0.001$ in every case).

Table 3. *Widths of the surface projections of three coronaviruses determined using different negative stains*

Coronavirus species	Potassium phosphotungstate widths (nm)[a]				Uranyl acetate widths (nm)[b]			
	Number of observations	Mean	Standard error	Range	Number of observations	Mean	Standard error	Range
IBV Conn	75	9.6	0.18	6.2—13.0	63	10.5	0.16	7.4—13.0
HCV 229E	90	8.7	0.09	5.8—10.5	66	9.8	0.17	7.7—13.0
MHV3	91	5.1	0.07	3.1—7.0	53	5.5	0.16	2.7—8.2

[a] Negative staining with 2 per cent potassium phosphotungstate, pH 6.5
[b] Negative staining with 0.5 per cent uranyl acetate, pH 4.4

Effect of Purification on Virus Morphology

Virus particles were also examined from partially purified samples in order to see if our purification procedure had had any effect on the virus morphology. Unfortunately, too few particles were present in crude clarified preparations to enable an accurate study to be made of them. However, pelleted virus preparations, before sucrose density gradient centrifugation, had sufficient virus particles present for analysis, although many of them were at least partially obscured by cell debris in MHV3 preparations. Essentially no difference was observed in the morphology of the three coronavirus species between partially purified pelleted and purified virus particles, suggesting that our purification procedure has little effect on virus morphology.

Discussion

The sizes of coronaviruses reported in the literature (15) vary widely, but it has not been clear how much of the variation was due to different methods of preparation, purification and negative staining, and whether different coronavirus species really do vary in size. Our results show that IBV Conn particles are much larger than those of HCV 229E and MHV3, and these may reflect significant molecular differences in their structures. In this respect it is interesting to note that the polypeptide compositions of IBV particles (11, 14) show significant differences from the polypeptide compositions of HCV (5, 6, 9) and MHV (9, 19, 20), although the RNA genomes of IBV (8, 12, 17) and HCV (13, 21) show close similarities.

Most reports on coronavirus morphology, summarised by McIntosh (15), have suggested that coronavirus particles have only one type of surface projection, the typical bulbous or 'tear-drop' shaped projection. However, a few reports (1, 3, 4, 16) have indicated the existence of another type of surface projection that is rod-shaped and sometimes has a spherical dilation or T-shaped structure at the distal end. Apparently, IBV (2, 3, 4) and haemagglutinating encephalomyelitis virus (16) particles can have different types of surface projections, whilst other coronavirus species have one or other type of surface projection. The bulbous HCV 229E and 'cone-shaped' MHV3 surface projections do not seem to consist of fundamentally different polypeptides as they are composed of glycopolypeptides

of similar size (MACNAUGHTON, unpublished results). However, the surface projections of IBV Conn are morphologically unlike those of MHV3 and only superficially similar to those of HCV 229E, and the IBV glycopolypeptides (14) are distinctly different from those of the other two viruses.

It is difficult to understand why the morphology of the surface projections is different. The differences cannot be attributed to staining procedures as identical methods were used for all three coronaviruses. The widely spaced typical bulbous coronavirus projections of IBV Conn and HCV 229E may reflect aggregations of the thinner, cone-shaped, MHV3-like projections which are more closely packed. This would explain how we have occasionally observed surface projections of different morphology in HCV 229E and MHV3 preparations. Similarly, it would clarify previous reports that have shown certain coronavirus preparations to contain atypical surface projections. However, the different surface projections may be made up of similar glycopolypeptides that are arranged slightly differently, producing a different morphology, but exhibiting similar biological functions. It has been shown that staining virus particles with UA can vary the morphology of the projections of all three coronavirus species and the envelope diameters of HCV 229E and MHV3. However, the action of UA as a negative stain is not understood. One suggestion is that UA is acidic and its reaction with polypeptides may depend on their isoelectric points (7).

It is important to determine how great is the morphological variation exhibited by coronavirus species and to establish whether such differences can be related to their biochemical structures. In this way it should be possible to establish whether such variations are significant and whether the coronavirus group should be subdivided.

Acknowledgments

We wish to thank Miss M. H. Madge for preparation of the viruses and Dr. R. R. Dourmashkin, Dr. M. V. Nermut, Dr. S. Patterson and Dr. D. A. J. Tyrrell for their advice and Dr. I. D. Hill for help with the statistics.

References

1. CAUL, E. O., EGGLESTONE, S. I.: Further studies on human enteric coronaviruses. Arch. Virol. **54**, 107—117 (1977).
2. COLLINS, M. S., ALEXANDER, D. J., HARKNESS, J. W.: Heterogeneity of infectious bronchitis virus grown in eggs. Arch. Virol. **50**, 55—72 (1976).
3. ESTOLA, S., WECKSTRÖM, P.: Electron microscopy of infectious bronchitis virus. Ann. Med. exp. Biol. Fenn. **45**, 30—31 (1967).
4. HARKNESS, J. W., BRACEWELL, C. D.: Morphological variation among avian infectious bronchitis virus strains. Res. vet. Sci. **16**, 128—131 (1974).
5. HIERHOLZER, J. C.: Purification and biophysical properties of human coronavirus 229E. Virology **75**, 155—165 (1976).
6. HIERHOLZER, J. C., PALMER, E. L., WHITFIELD, S. G., KAYE, H. S., DOWDLE, W. R.: Protein composition of coronavirus OC43. Virology **48**, 516—527 (1972).
7. JOHANSEN, B. V., HØGLUND, S.: Report on a symposium on contrast problems in transmission electron microscopy. Ultramicroscopy **1**, 83—87 (1975).
8. LOMNICZI, B., KENNEDY, I.: Genome of infectious bronchitis virus. J. Virol. **24**, 99—107 (1977).
9. MACNAUGHTON, M. R.: A comparison of the polypeptides of human and mouse coronaviruses. Submitted for publication.

10. Macnaughton, M. R., Davies, H. A., Nermut, M. V.: Ribonucleoprotein-like structures from coronavirus particles. J. gen. Virol. **39**, 545—549 (1978).
11. Macnaughton, M. R., Madge, M. H.: The polypeptide composition of avian infectious bronchitis virus particles. Arch. Virol. **55**, 47—54 (1977).
12. Macnaughton, M. R., Madge, M. H.: The characterisation of the virion RNA of avian infectious bronchitis virus. FEBS Letts. **77**, 311—313 (1977).
13. Macnaughton, M. R., Madge, M. H.: The genome of human coronavirus strain 229E. J. gen. Virol. **39**, 497—504 (1978).
14. Macnaughton, M. R., Madge, M. H., Davies, H. A., Dourmashkin, R. R.: Polypeptides of the surface projections and the ribonucleoprotein of avian infectious bronchitis virus. J. Virol. **24**, 821—825 (1977).
15. McIntosh, K.: Coronaviruses: A comparative review. Curr. Top. Microbiol. Immunol. **63**, 85—129 (1974).
16. Pocock, D. H.: Effect of sulphydryl reagents on the biological activities, polypeptide composition and morphology of haemagglutinating encephalomyelitis virus. J. gen. Virol. **40**, 93—101 (1978).
17. Schochetman, G., Stevens, R. H., Simpson, R. W.: Presence of infectious polyadenylated RNA in the coronavirus avian bronchitis virus. Virology **77**, 772—782 (1977).
18. Song, S. K., Shimada, N., Anderson, P. J.: Orthoganol diameters in the analysis of muscle fibre size and form. Nature **200**, 1220—1221 (1963).
19. Sturman, L. S.: Characterization of a coronavirus. I. Structural proteins: effects of preparative conditions on the migration of protein in polyacrylamide gels. Virology **77**, 637—649 (1977).
20. Sturman, L. S., Holmes, K. V.: Characterization of a coronavirus. II. Glycoproteins of the viral envelope: tryptic peptide analysis. Virology **77**, 650—660 (1977).
21. Tannock, G. A., Hierholzer, J. C.: The RNA of human coronavirus OC-43. Virology **78**, 500—510 (1977).
22. Tyrrell, D. A. J., Almeida, J. D., Berry, D. M., Cunningham, C. H., Hamre, D., Hofstad, M. S., Mallucci, L., McIntosh, K.: Coronaviruses. Nature **220**, 650 (1968).

Authors' address: Dr. M. R. Macnaughton, Division of Communicable Diseases, Clinical Research Centre, Watford Road, Harrow, Middlesex HA1 3UJ, England.

Received June 30, 1978